Phys. Status Solidi C **12**, No. 4–5, 460–465 (2015) / **DOI** 10.1002/pssc.201400200

physica status solidi c
www.pss-c.com
current topics in solid state physics

Computational model of 2DEG mobility in AlGaN/GaN heterostructures

Karine Abgaryan[*,1], **Ilya Mutigullin**[1], **and Dmitry Reviznikov**[2]

[1] Dorodnicyn Computer Center of RAS, Vavilov st. 40, 119333 Moscow, Russia
[2] Moscow Aviation Institute, Volokolamskoe Shosse 4, 125993 Moscow, Russia

Received 31 July 2014, revised 5 January 2015, accepted 4 February 2015
Published online 3 March 2015

Keywords III-V nitrides, semiconductors, heterostructures, computational modeling.

[*] Corresponding author: e-mail kristal83@mail.ru

The computational scheme of multiscale modeling of semiconductor heterostructures is presented. Three scale levels are taken into account. On the atomic level the system is described using crystallographic information and quantum-mechanical model. *Ab initio* modeling allows to determine the electronic structure, define polarization effects and calculate charge densities on the interfaces between layers. Obtained information is used in the nanoscale level model for the calculation of the charge carrier distribution in the heterostructure. At this level mathematical model contains the system of conjugated Schrödinger and Poisson equations. The carrier density distributions over the lateral direction of the multilayered structure and 2DEG localization are of the most interest at this point. This data is used in the next scale level model where electron mobility is calculated. A wide range of electron scattering mechanisms are taken into account during this calculation. This approach was applied to model 2DEG in AlGaN/AlN/GaN heterostructures. The good agreement between calculated values of interface charge density, 2DEG electron concentration, electron mobility and known experimental data was achieved.

1 Introduction The tendency of miniaturization of device dimensions as well as maximization of charge carrier concentrations with maximum mobility is the modern trend of the high-frequency semiconductor technics development. For that purpose multilayered nanoscale heterostructures with two-dimensional electronic gas are used. The main factors affecting the origin of carriers transport channels (2DEG) in the vicinity of heterointerface are the concentration of dopants in the barrier layer and the presence of the surface charge on the interface. Latter is typical for wurtzite structures and is determined by spontaneous and piezoelectric polarization.

There were a lot of papers on mathematical modeling of heterostructures. The detailed description of various computational aspects of carrier concentration and mobility simulation can be found in [1-5]. The analysis of known theoretical and experimental data shows the importance of taking into account various factors on different scale levels such as lattice mismatch between layers, spontaneous and piezoelectric polarization, conduction bands shifts, barrier layer doping, interface roughness, etc. This is the reason of the significance of interrelated consideration of various effects on different scale levels which is the topic of the present paper.

2 Multi-scale modeling scheme

The scheme of multi-scale semiconductor heterostructure modeling was developed in Dorodnicyn Computing Centre of RAS. The scheme is shown in Fig. 1.

Three significant scale levels are taken into account. On the atomic level the system is described using crystallographic information and *ab initio* calculations performed in the framework of Density functional theory. First-principles modeling allows to determine electronic structure and basic properties of heterostructure, define polarization effects and calculate charge densities on the interfaces between layers.

First principles calculations of the polarization properties of semiconductors AlN, GaN and AlGaN with wurtzite structures were performed in the framework of DFT using the Berry phase approach [6, 7]. DFT calculations were carried out using both the local density approximation

(LDA) and generalized gradient approximation (GGA) of exchange-correlation functional. Our calculations were performed using Vienna *Ab-initio* Simulation Package (VASP) [8, 9] based on pseudopotentials and a plane-wave basis set to solve the Kohn–Sham equations with periodic boundary conditions. The results of these calculations were presented in our previous paper [10]. The values of the spontaneous and the piezoelectric polarization and the piezoelectric constants were calculated for these nitride compounds. The obtained values of the spontaneous and piezoelectric polarizations allowed to calculate the bound interface charge densities were calculated for AlN/GaN, AlGaN/AlN, AlGaN/GaN interfaces. The obtained values of the bound charge densities at the different interfaces are as follows: (AlN/GaN) = 6.79×10^{13} cm^{-2}; (AlGaN/AlN) = -5.44×10^{13} cm^{-2}; (AlGaN/GaN) = 1.35×10^{13} cm^{-2}.

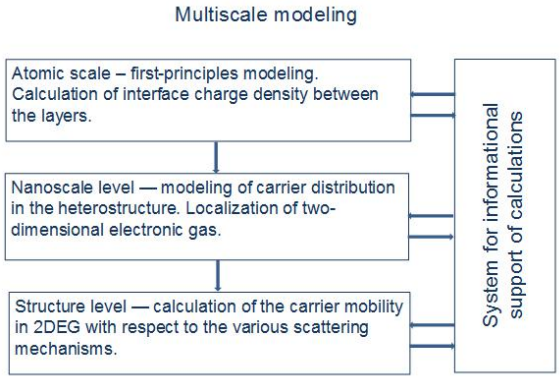

Figure 1 Multiscale modelling scheme.

The results of modeling on the atomic scale level is used in the nanoscale level model for the calculation of the charge carriers distribution in the heterostructure. At this level the mathematical model contains the system of conjugated Schrödinger and Poisson equations.

$$-\frac{\hbar^2}{2}\nabla\left(\frac{1}{m^*}\nabla\psi\right)+(-e\phi+\Delta E_c)\psi=E\psi\,, \quad (1)$$

$$\nabla(\varepsilon\nabla\phi)=-e(N_D-N_A-n)+\sum_l\sigma_l\delta(z-z_l)\,, \quad (2)$$

$$n(r)=\sum_i\psi_i^*(r)\psi_i(r)n_i\,, \quad (3)$$

$$n_i=k_BT\frac{m^*}{\pi\hbar^2}\ln\left(1+\exp\left(\frac{E_F-E_i}{k_BT}\right)\right), \quad (4)$$

here E_i and $\psi_i(r)$ are energetic levels and corresponding wavefunctions, $n(r)$ - electron concentration, $\hbar$ - Dirac constant, e - electron charge, m^* - effective electron mass, E_F - Fermi level, $\varphi(r)$ - Coulomb potential, $V(r)$ - potential energy of a carrier, N_D, N_A - concentrations of donor and acceptor dopants, σ - interface charge densities, δ - delta-function, z_l - coordinates of interfaces, ε - dielectric constant, k_B - Boltzmann constant, T - temperature.

The use of the concept of electron effective mass allows us to avoid the detailed consideration of the interaction between electrons and nucleus. As a result it is possible to shift the view from atomic level to the nanoscale level of real heterostructures. The carrier density distribution across the multilayered structure and localization of the area of increasing concentration (2DEG) are of the most interest.

Computational modeling is performed using finite-difference approximation and subsequent solution of discrete analogs. It is characteristic for the heterostructures in which quantum confinement is achieved via barrier layer doping that the Poisson's equation contains distributed source. In wurtzite type structures spontaneous and piezoelectric polarization appear. As a result there is charge concentration on the boundary between different layers. This leads to the localized sources and the need in high resolution of computational grid.

Local computational procedures aimed to solve Schrödinger and Poisson equations are integrated by global iterative process which makes their solutions consistent. Computational process can be described schematically as follows. The right part of the Poisson equation is calculated using the electron distribution information obtained at last iteration. New Coulomb potential and potential energy distribution are calculated. Schrödinger equation is solved using this information. As a result significant energy levels and corresponding grid wavefunctions are obtained. They are used to calculate new distribution of electron concentration in the system. The process is repeated until convergence is achieved. Convergence of iterative process is regulated by relaxation parameter. Strong link between equations is characteristic for this class of problems. This leads to the problem of convergence of the iterations. It is necessary to use under-relaxation with rather small relaxation parameter to achieve convergence. To improve convergence process we apply the approach based on the local approximation of implicit dependence of carrier concentration on the potential [11]. It is of the form

$$n(\varphi)\approx\sum_i\psi_i^*\psi_i\,k_BT\frac{m^*}{\pi\hbar^2}\ln\left(1+\exp\left(\frac{E_F-E_i+e(\varphi-\varphi^{(k)})}{k_BT}\right)\right) \quad (5)$$

here $\varphi(k)$ is the potential, obtained on the previous iteration of the global process.

This leads to the modified Poisson equation with explicit nonlinearity:

$$\nabla(\varepsilon\nabla\varphi)=-e(N_D-N_A-n(\varphi))+\sum_l\sigma_l\delta(z-z_l)\,. \quad (6)$$

To solve modified Poisson equation the linearization is used in the form

$$\phi=\phi^{(p)}+\xi\,, \quad (7)$$

$$\nabla(\varepsilon\nabla\xi)=g\xi+q\,, \quad (8)$$

$$g=e\frac{\delta n}{\delta\phi}(\phi^{(p)})\,, \quad (9)$$

$$q = -\nabla(\varepsilon\nabla\phi^{(p)}) + (-e(N_D - N_A - n(\phi^{(p)})) + \sum_l \sigma_l \delta(z - z_l) \qquad (10)$$

In Fig. 2 the convergence of iterative process typical for heterostructures under consideration is illustrated. Shown are the results for the case thoroughly analyzed below. Curve 1 here corresponds to the under-relaxation method, curve 2 corresponds to the local approximation of carrier concentration as a function of potential (under-relaxation is not required in this case). It can be seen that the acceleration of convergence is significant, in this particular case 40 iterations as opposed to more than 200 iterations.

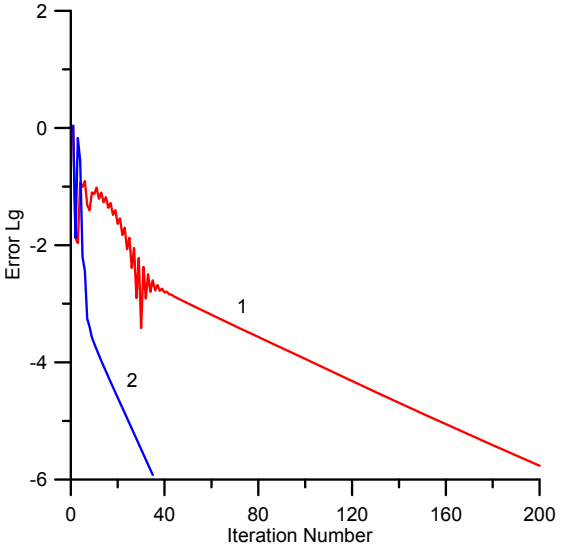

Figure 2 Convergence of global iterations.

Because it is necessary to solve Schrödinger and Poisson equations at each global iteration the efficiency of computational process to a large extent depends on the effectiveness of the algorithms of their solution. Therefore accounting of the positions of significant energy levels is very important. According to Fermi-Dirac statistics the electrons on the lowest energy levels contribute to the increasing of carriers concentration in 2DEG. Information about the lower limit is obtained during the Poisson equation solution on current iteration. Consequently, the bisection method in combination with inverse iterations are effective for the Schrödinger equation solution.

Numerical experiments have shown that our approach provides high efficiency on rather fine grids for both distributed and localized charge sources.

The data obtained as a result of self-consistent solution of Schrödinger and Poisson equations is used in the next scale level model. In this model the calculation of carrier mobility is performed. The wide range of scattering mechanisms is taken into account: scattering on optical and acoustical phonons, on heterostructure roughness, on charge centers and dislocations, piezoelectric scattering.

3 Modeling results

As an example of an approach under development let us consider the modeling of semiconductor heterostructure [12], grown by vapour deposition method (Fig. 3, taken from [12]). The combination of barrier layer doping (area source in Poisson equation) and uncompensated interface charge because of spontaneous and piezoelectric polarization (localized sources) is typical for this kind of structure. GaN layer on the surface of barrier layer prevents it's oxidation. AlN layer accounts for the decrease of alloy scattering which only exists in ternary alloys and alloys consisting of more than three components. As a result the electrons which penetrate the barrier because of the existence of density of states tail under the barrier with finite height do not scatter on the alloy potential. Input data for calculations were taken from [12].

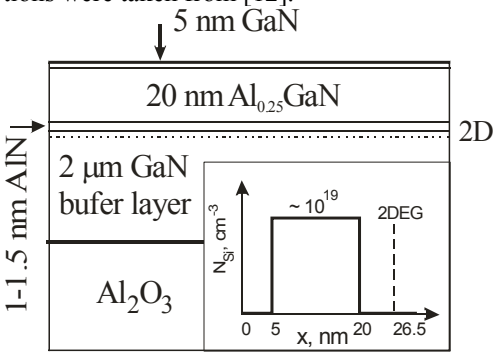

Figure 3 AlGaN/AlN/GaN heterostructure under consideration. The properties of this structure are discussed in detail in [12].

The following values of charge density on interfaces are achieved as the results of our calculations:

$$\frac{\sigma}{e}(AlGaN/AlN) = -5.71\ \mathrm{cm}^{-2},$$

$$\frac{\sigma}{e}(AlN/GaN) = 6.79\mathrm{cm}^{-2},$$

$$\frac{\sigma}{e}(AlGaN/GaN) = 1.08\mathrm{cm}^{-2}.$$

The results of self-consistent solution of Schrödinger and Poisson equations obtained using data from ab initio modeling are shown in Fig. 4 and 5. Blue curves labeled 1 (related to the left scale) in parts (a) of the figures demonstrate the potential energy profile, while red curves labeled 2 (right scale) demonstrate electron concentration distribution over the thickness of the heterostructure. Horizontal dashed lines indicate the two lower electron energy levels. Part (b) figures demonstrate the corresponding electron wavefunctions. Curves 1, 2 and 3 in parts (b) of the figures correspond to the three lowest energy levels while dashed curves are Fang-Howard analytical functions. Results de-

picted in the Fig. 4 are obtained by ignoring the conduction bands shift between AlN and AlGaN. Results in the Fig. 5 are obtained with taking this shift into account. The small discrepancy in the behavior of wave functions and carrier concentration distribution in the vicinity of heterointerface is noticeable. Taking into account of the shift leads to the less prominent penetration of barrier layer by electrons. At the same time the difference between total electron concentrations in 2DEG is negligible, about 1%. Obtained concentration (1.02×10^{13} cm^{-2}) is in a good agreement with experimental data [12].

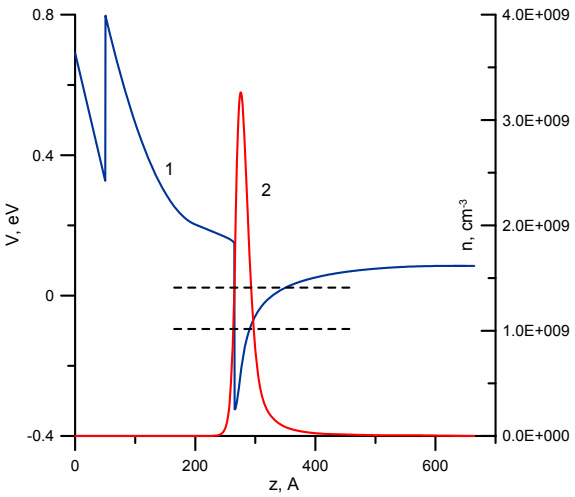

Figure 4a Electron concentration and potential energy distribution over the AlGaN/AlN/GaN heterostructure. Results are obtained by ignoring the conduction bands shift between AlN and AlGaN. The peak in the red curve corresponds to the 2DEG position.

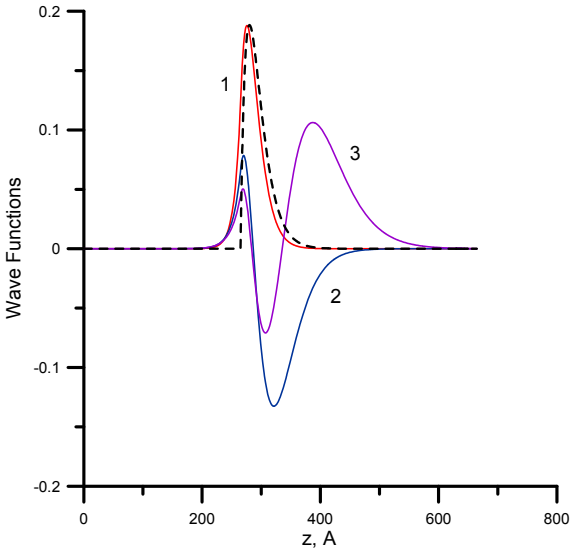

Figure 4b Wavefunctions in the AlGaN/AlN/GaN heterostructure. Results are obtained by ignoring the conduction bands shift between AlN and AlGaN.

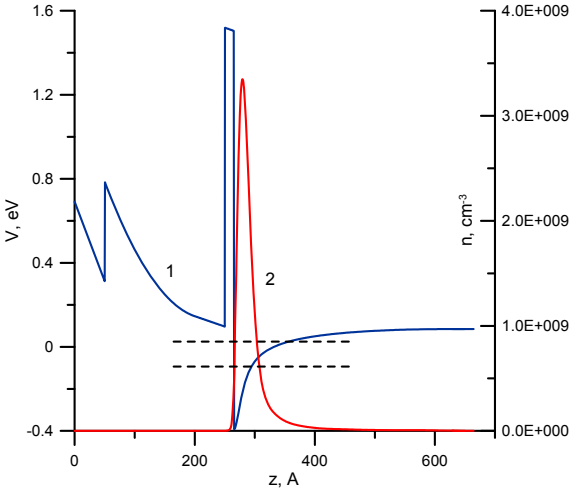

Figure 5a Electron concentration and potential energy distribution over the AlGaN/AlN/GaN heterostructure. Results are obtained by taking the conduction bands shift between AlN and AlGaN into account. The peak in the red curve corresponds to the 2DEG position.

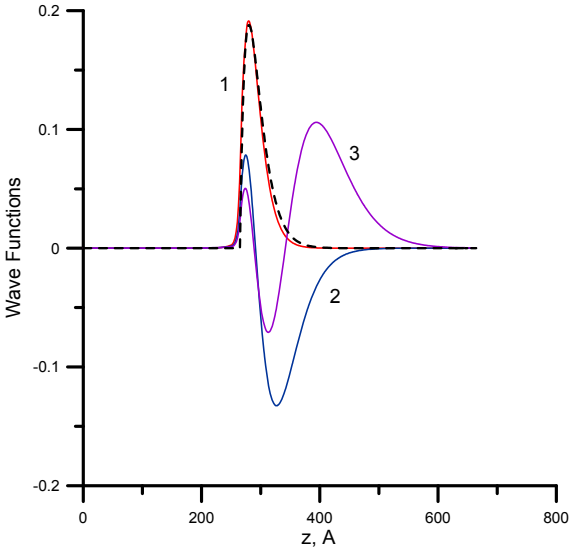

Figure 5b Wavefunctions in the AlGaN/AlN/GaN heterostructure. Results are obtained by taking the conduction bands shift between AlN and AlGaN into account.

It is worth mentioning that the first wave function in Fig. 4 (and especially in Fig. 5) is in a good agreement with a well-known analytical Fang-Howard function [13] $\psi(z) = \left(b^3/2\right)^{1/2} z \exp(-bz/2)$ (dashed curves in the parts (b) of the figures).

Energy levels and corresponding wave functions obtained from the self-consistent solution of Schrödinger and Poisson equations are used to calculate electron mobility in the direction length-wise with respect to the heterointerface. It is necessary to take into account different scattering mechanisms. We use well-known formulas for the scattering rate and the Mattiessen's rule which allows to deter-

mine the total relaxation time and electron mobility using the rates of different scattering mechanisms [12, 14, 15]. The results of the comparison of calculated and experimental data are shown in Fig. 6 and 7. Mobility dependences on carrier densities in 2DEG at different temperatures and mobility dependence on temperatures at concentration 10^{13} cm^{-2} are presented. The effects of various scattering mechanisms were analyzed in [12] and the conclusion was made that for the structure under consideration the most important scattering mechanisms are: scattering on optical phonons – at room temperature, and scattering at dislocations, surface roughness and alloy inhomogeneity – at low temperatures. This is the reason for the qualitative difference between the curves in case of 300 K (Fig. 6a) and 77 K (Fig. 6b). It is clear that the application of fitting procedures is necessary here because some of the parameters (e.g. dislocation concentration, interface roughness data) are not directly measured. Nevertheless, the implementation of fitting at one point (at one temperature and at one concentration) allows us to reproduce experimental dependences at the temperature and concentration ranges under consideration.

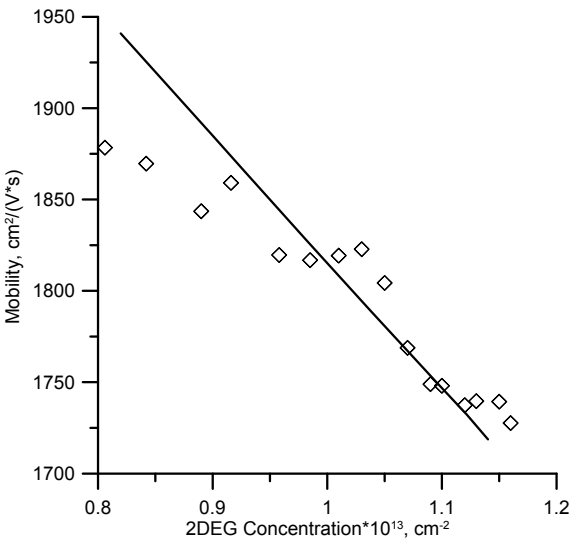

Figure 6a Dependence of mobility on concentration at 300 K. The rhombic dots represent experimental values from [12] while solid line corresponds to the results of our calculation.

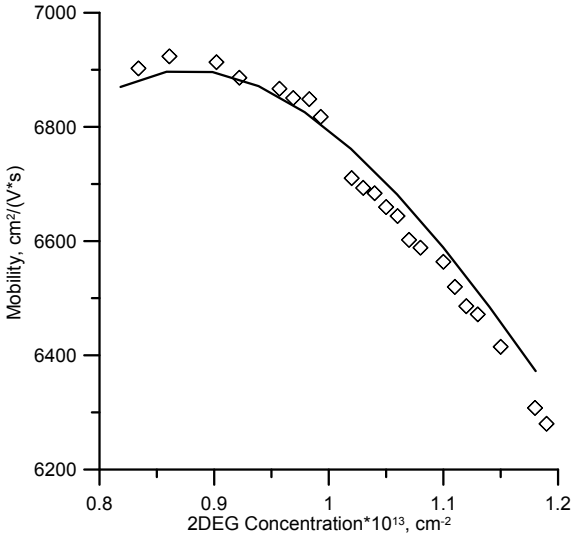

Figure 6b Dependence of mobility on concentration at 77 K. The rhombic dots represent experimental values from [12] while solid line corresponds to the results of our calculation.

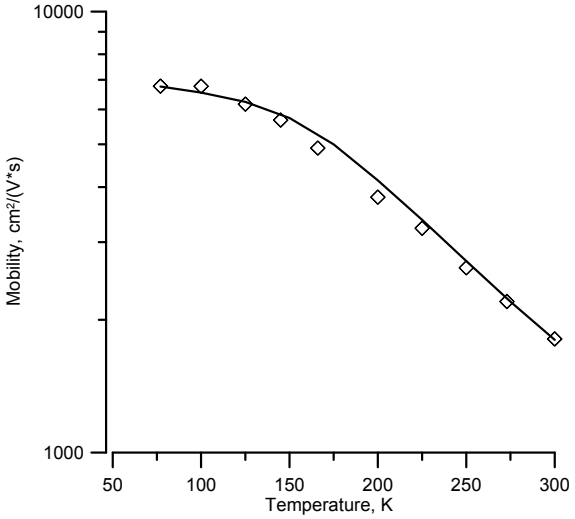

Figure 7 Dependence of mobility on temperature. The rhombic dots represent experimental values from [12] while solid line corresponds to the results of our calculation.

4 Summary The computational multi-scale scheme for semiconductor heterostructure properties modeling is presented. The data obtained from atomic level calculations is used in the nanoscale level calculation of the carriers distribution in the heterostructure. And on the next step the electron mobility is calculated with respect to a wide range of scattering mechanisms. Obtained results are in a good agreement with known experimental results.

References

[1] D. Vasileska, S. M. Goodnick, and S. Goodnick, Computational Electronics: Semiclassical and Quantum Device Modeling and Simulation (CRC Press, 2010).
[2] K. Tomizawa, Numerical Simulation of Submicron Semiconductor Devices (Artech House Inc., Japan, 1993).
[3] Z. Yarar, B. Ozdemir, and M. Ozdemir, Phys. Status Solidi B **242**, 2872 (2005).
[4] D. K. Ferry, S. M. Goodnick, and J. Bird, Transport in Nanostructures (Cambrige University Press, 2009), p. 659.
[5] O. Ambacher, J. Majewski, C. Miskys, A. Link, M. Hermann, M. Eickhoff, M. Stutzmann, F. Bernardini, V. Fiorentini, V. Tilak, B. Schaff, and L. F. Eastman, J. Phys.: Condens. Matter **14**, 3399 (2002).
[6] R. D. King-Smith and D. Vanderbilt, Phys. Rev. B **47**, 1651 (1993).
[7] R. Resta, Rev. Mod. Phys. **66**, 899 (1994).
[8] G. Kresse and J. Furthmüller. Phys. Rev. B **54**, 11169 (1996).
[9] G. Kresse and D. Joubert. Phys. Rev. B **59**, 1758 (1999).
[10] I. Supryadkina, K. Abgaryan, D. Bazhanov, and I. Mutigullin, Phys. Status Solidi C **11**, 307 (2014)
[11]. A. Trellakis, A. T. Galick, A. Pacelli, and U. Ravaioli, J. Appl. Phys. **81**, 12 (1997).
[12] D. Yu. Protasov, T. V. Malin, A. V. Tikhonov, A. F. Tsatsulnikov, and K. S. Zhuravlev, Semiconductors **47**, 33 (2013).
[13] F. F. Fang and V. E. Howard, Phys. Rev. Lett. **16**, 797 (1966).
[14] L. Hsu and W. Walukiewicz, Phys. Rev. B **56**, 1520 (1997).
[15] J. F. Zhang, Y. Hao, J. C. Zhang, and J. Y. Ni, Sci. China F **51**, 780 (2008).